Springer

KSME

Journal of Mechanical Science and Technology 24 (4) (2010) 983~990
www.springerlink.com/content/1738-494x
DOI 10.1007/s12206-010-0216-8

Numerical study on leakage detection and location in a simple gas pipeline branch using an array of pressure sensors †

Sung Pill Jang, Chan Young Cho, Jin Hyun Nam*, Si-Hyung Lim, Donghoon Shin and Tae-Yong Chung

School of Mechanical and Automotive Engineering, Kookmin University, Seoul, 136-702, Korea

(Manuscript Received September 4, 2009; Revised January 18, 2010; Accepted January 20, 2010)

Abstract

Pressure signals measured in gas pipelines provide useful information for monitoring the status of pipeline network operations. This study numerically investigates leakage detection and location in a simple gas pipeline branch using transient signals from an array of pressure sensors. A pipeline network simulation model was developed and used to predict one-dimensional compressible flow in gas pipelines. Two monitoring methods were tested for leakage detection and location; these include cross-correlation monitoring and pressure differential monitoring. The performance and reliability of the two monitoring methods were numerically assessed based on simulation results for a simple pipeline branch operation with a prescribed leakage rate (5% of total flow rate in the gas pipeline).

Keywords: Pipeline network; Leakage detection; Numerical analysis; Compressible flow; Cross-correlation

1. Introduction

Pipeline networks used for supplying natural gas have become increasingly complex in accordance with the rising natural gas usage for industrial and household use. Natural gas pipelines are exposed to risks of leakage due to gradual corrosion of pipe materials over time and the unexpected damage of pipe structures upon natural and artificial accidents. Therefore, detection and location of leakage has become essential in the safe operation of natural gas pipelines [1].

Current leakage detection technologies can be classified as biological, hardware-based, and software-based methods [2]. Biological detection relies on trained personnel or animals in sensing leaked substances. More precise devices like acoustic sensors, visual devices, and gas sampling devices are utilized in the hardware-based detection [3]. In contrast, software-based detection monitors flow rate, pressure, and temperature data from a supervisory control and data acquisition (SCADA) system. Based on the difference between measured state variables and calculated variables, the status of pipeline networks is checked, after which possible leakage is detected by the software -based method [4-9].

Advancements in sensor network technologies have led to a new concept of distributed pipelines monitoring [10]. While the SCADA system conducts global centralized monitoring of pipeline networks, each distributed system performs autonomous monitoring of a certain localized region at higher risks, such as an exposed pipe installed on bridges. A distributed system should be able to judge the operational status of its monitored region and send abstracted information to the central SCADA system. Thus, a simple method that does not require much computational resource is essential for distributed pipeline monitoring.

An array of pressure sensor is promising in the detection and location of possible leakage in simple gas pipeline branches. Pressure sensors are easier to install and require lower cost for maintenance, compared with flow rate sensors. In addition, transient signals from pressure sensors can be readily incorporated into the central SCADA system as additional monitoring data. Therefore, this study numerically investigates the possibility of leakage detection and location in a simple pipeline branch using transient signals from a pressure sensor array.

A pipeline network simulation model was developed and validated for accurate prediction of one-dimensional compressible flow in gas pipelines. Two monitoring methods based on pressure sensor signals were tested for leakage detection and location, namely, cross-correlation monitoring and pressure differential monitoring. The performance and reliability of the two detection methods were assessed based on the simulation results from a simple pipeline branch operation with a prescribed leakage rate (5% of total flow rate in the pipeline).

† This paper was recommended for publication in revised form by Associate Editor Won-Gu Joo
*Corresponding author. Tel.: +82 2 910 4858, Fax.: +82 2 910 4839
E-mail address: akko2@kookmin.ac.kr

2. Theory and calculation

2.1 Governing equation

The governing equations for pressure p (Pa) and flow rate q (m^3/s) in gas pipelines are summarized [11-14]:

$$\frac{\partial q}{\partial x} = -\frac{A}{\rho a^2}\frac{\partial p}{\partial t}, \tag{1}$$

$$\frac{\partial p}{\partial x} = -\frac{\rho}{A}\frac{\partial q}{\partial t} - \frac{f\rho q|q|}{2DA^2} - \rho g \sin\alpha, \tag{2}$$

where ρ is the density of gas, a is the speed of sound, A and D are the cross-sectional area and the diameter of a pipe, f is the Darcy friction factor, and α is the slope angle of the pipe ($\alpha = 0$ is assumed in this study).

Eqs. (1) and (2) are derived from the continuity and the Navier-Stokes equations for one-dimensional compressible flow in pipes by assuming an isothermal process of ideal gas. Thus, the speed of sound is determined as $a = \sqrt{p/\rho} = \sqrt{RT}$. The friction factor f for a pipe can be estimated utilizing the Colebrook equation [15],

$$\frac{1}{\sqrt{f}} = -1.0\log\left(\frac{\varepsilon/D}{3.7} + \frac{2.51}{\mathrm{Re}\sqrt{f}}\right). \tag{3}$$

when gas flows along a pipeline at a constant mass flow rate $\dot{m}$, the flow rate denoted by q in Eqs. (1) and (2) can be varied according to gas density ρ. To avoid such numerical inconvenience, a normalized flow rate q_n (Nm^3/s) is introduced, where q_n denotes the flow rate at the normal condition of $p_n = 1$ bar and $T_n = 288$ K. Then, Eqs. (1) and (2) can be rearranged in terms of q_n using $\dot{m} = \rho q = \rho_n q_n$:

$$\frac{\partial q_n}{\partial x} = -\frac{A}{\rho_n a^2}\frac{\partial p}{\partial t}, \tag{4}$$

$$\frac{\partial p}{\partial x} = -\frac{\rho_n}{A}\frac{\partial q_n}{\partial t} - \frac{f\rho_n q_n|q_n|p_n}{2DA^2 p}. \tag{5}$$

Note that all numerical simulations were based on Eqs. (4) and (5). Thus, normalized flow rate q_n can be regarded as a main variable in the remaining part of this paper.

2.2 Finite volume discretization

2.2.1 Simple pipeline branch

The spatial discretization procedure for a simple pipeline branch is explained in Fig. 1. Pipeline length L is divided into N sub-sections with uniform length $\Delta L = L/N$, and then the nodes for pressure calculation p_i are placed at each interface between two sub-sections. Similarly, the nodes for flow rate calculation $q_{n,i}$ are placed in the middle of each sub-section. Thus, the total number of pressure nodes is $N+1$ ($p_1 \cdots p_{N+1}$) while that of flow rate nodes is N ($q_{n,1} \cdots q_{n,N}$).

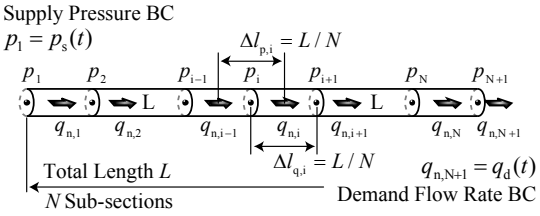

Fig. 1. Spatial discretization of a simple pipeline branch.

Note that the grid structure shown in Fig. 1 is similar to staggered grids commonly used in computation fluid dynamics (CFD). Flow rate nodes are located between every two pressure nodes (e.g., $q_{n,i}$ denotes the flow rate from p_i to p_{i+1}). Thus, flow rate is defined as positive when gas flows from an upstream supply side in the left to a downstream demand side in the right.

By integrating Eqs. (4) and (5) for finite volumes, as shown in Fig. 1, the following discretized equations are obtained:

$$\frac{q_{n,i} - q_{n,i-1}}{\Delta l_{p,i}} = -\frac{A}{\rho_n a^2}\frac{p_i - p_i^o}{\Delta t}, \tag{6}$$

$$\frac{p_{i+1} - p_i}{\Delta l_{q,i}} = -\frac{\rho_n}{A}\frac{q_{n,i} - q_{n,i}^o}{\Delta t} - \frac{f\rho_n}{2DA^2} q_{n,i}|q_{n,i}|\frac{p_n}{\bar{p}_i}. \tag{7}$$

Here, Δt is the time step, p_n is the normal pressure (1 bar), and $\Delta l_{p,i}$ and $\Delta l_{q,i}$ are the control lengths for pressure node p_i and flow rate node $q_{n,i}$, respectively. Note that internal pressure nodes have $\Delta l_{p,i} = \Delta L$ while boundary nodes have $\Delta l_{p,i} = \Delta L/2$. Average pressure $\bar{p}_i$ denotes the mean pressure at flow rate node $q_{n,i}$ and thus calculated as $\bar{p}_i = (p_i + p_{i+1})/2$. The implicit Euler scheme is used for temporal discretization.

Two boundary conditions (BCs) are required for the solution of Eqs. (6) and (7). A prescribed pressure BC is generally given at the upstream supply side as $p_1 = p_s(t)$, while a prescribed flow rate BC is given at the downstream demand side as $q_{n,N+1} = p_s(t)$.

2.2.2 Pipeline branch intersection (leakage)

Actual gas pipelines are composed of many simple pipeline branches that are cross-connected to form complex pipeline networks. Thus, consideration is required for branch intersections where more than three simple pipeline branches meet, as shown in Fig. 2. Note that this consideration is also essential in the modeling of leakage in a simple pipeline branch.

Since pressure nodes are placed at the end of each pipeline branch (Fig. 2), flow rate nodes always interact with pressure nodes in the same branch. Thus, Eq. (7) can be used without modification. However, for pressure node p_i located at the intersection point in Fig. 2, Eq. (6) should be modified [11] as

$$q_{n,i\to j}^1 + q_{n,i\to j}^2 + q_{n,i\to j}^3 = -\frac{A}{\rho_n a^2}\frac{p_i - p_i^o}{\Delta t}\Delta l_{p,i}, \tag{8}$$

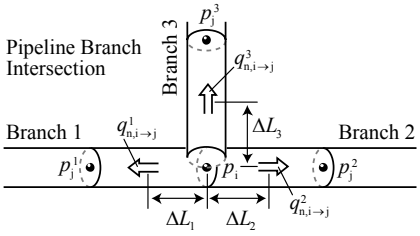

Fig. 2. Spatial discretization for a pipeline branch intersection.

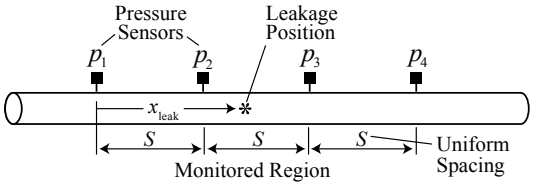

Fig. 3. Leakage detection and location using four pressure sensors installed in a simple pipeline branch.

where $q^{k}_{n,i\to j}$ denotes the flow rate from p_i to p^{k}_{j} in pipeline branch k, and $\Delta l_{p,i}$ denotes the control length for pressure node p_i, which is calculated as $\Delta l_{p,i} = \Delta L_1 + \Delta L_2 + \Delta L_3$.

For modeling of leakage at pressure node p_i in a simple pipeline branch, $q^{3}_{n,i\to j}$ in Eq. (8) should be substituted by a prescribed leakage flow rate q_{leak} while setting $\Delta L_3 = 0$.

2.3 Leakage detection method

Fig. 3 shows four pressure sensors, p_1, p_2, p_3, and p_4, installed in a simple pipeline branch with a uniform spacing of S. The monitored region is the $3S$ length of the pipeline enveloped by two outermost pressure sensors, p_1 and p_4. Leakage position x_{leak} is defined as the distance from the first pressure sensor. Two leakage detection methods considered in this study are explained below based on the configuration shown in Fig. 3.

2.3.1 Cross-correlation monitoring

Cross-correlation monitoring [16] is based on the cross-correlation coefficient that quantitatively measures the similarity of two signals. For two arbitrary signals, $s_1(t)$ and $s_2(t)$, cross-correlation coefficient $R_{s_1s_2}(\tau)$ is defined as [17, 18]

$$R_{s_1s_2}(\tau) = \frac{1}{T}\int_0^T s_1(t)s_2(t+\tau)\,dt\,, \tag{9}$$

where τ is the offset time and T is the integration period. When $s_1(t)$ and $s_2(t)$ show a similar behavior with a time delay of t_d, we see that $R_{s_1s_2}(\tau)$ has a peak value at $\tau = t_d$. Thus, abnormal signal sources between two pressure sensors can be detected and located by monitoring the cross-correlation coefficient of the two pressure sensor signals.

During the normal operation of a pipeline branch, temporal pressure variations $p'(\equiv \partial p/\partial t)$ recorded by the sensors are originated from external sources outside the monitored region (e.g., from upstream in the left or from downstream in the right). Thus, the cross-correlation coefficient of any two pressure sensor signals has its peak value when offset time τ equals the time of sound to travel the distance between the two sensors. For example, $R_{p'_1p'_3}(\tau)$ has its peak value at either $\tau = +2S/a$ for disturbed pressure signals from downstream or $\tau = -2S/a$ for those from upstream.

When unexpected leakage starts between p_1 and p_3 sensor locations, as shown in Fig. 3, two pressure variations measured by p_1 and p_3 sensors show a similar behavior at a time delay smaller than $2S/a$, resulting in a peak value of $R_{p'_1p'_3}(\tau)$ at $-2S/a < \tau < +2S/a$. Thus, leakage inside the monitored region can be detected by abnormally high peak values of $R_{p'_1p'_3}(\tau)$ compared with either $R_{p'_1p'_3}(-2S/a)$ or $R_{p'_1p'_3}(+2S/a)$. Once a leakage is detected, its position can be easily determined using peak offset time τ_{peak} for the peak value of $R_{p'_1p'_3}(\tau)$:

$$\frac{S+\Delta x}{a} - \frac{S-\Delta x}{a} = \tau_{peak}\,, \tag{10}$$

where Δx is the distance between the middle point of two sensors and the leakage position.

In summary, cross-correlation monitoring with two pressure sensors, p_i and p_j, can be stated as

$$\text{Detection:}\quad \frac{\text{peak}[R_{p'_ip'_j}(\tau)]}{\max[R_{p'_ip'_j}(\pm S_{ij}/a)]} > \text{TOL}\,, \tag{11}$$

$$\text{Location:}\quad \Delta x_{ij} = \frac{a\,\tau_{peak}}{2}\,, \tag{12}$$

where S_{ij} is the spacing between the two pressure sensors, Δx_{ij} is the distance between the middle point of two sensors and the leakage position, and TOL is the tolerance for leakage judgment.

2.3.2 Pressure differential monitoring

In pipes, pressure differential monitoring relies on the fluid dynamics relationship between pressure drop and flow rate. When gas pipelines are operated with relatively small temporal variation of flow rate ($\partial q_n/\partial t \approx 0$), Eq. (7) can be rearranged by $\overline{p}_i = (p_i + p_{i+1})/2$:

$$\frac{p_i^2 - p_{i+1}^2}{\Delta l_{q,i}} = -\frac{f\rho_n}{DA^2} q_{n,i}\left|q_{n,i}\right| p_n\,. \tag{13}$$

Note that the right hand side of Eq. (13) becomes almost constant for a simple pipeline branch without leakage. This is because the Darcy friction factor f, pipe dimensions D and A, and flow rate $q_{n,i}$ are rather uniform. Thus, Eq. (13) indicates that squared pressure p^2 linearly varies along a simple pipeline branch without leakage.

It can be inferred from Eq. (13) that squared pressure differences between any two neighboring sensors with a uniform

spacing S are almost the same when no leakage is present in the monitored region. This can be expressed by an equality of $p_1^2 - p_2^2 = p_2^2 - p_3^2 = p_3^2 - p_4^2$. However, when there is leakage inside the monitored region, as shown in Fig. 3, the equality is broken as $p_1^2 - p_2^2 > p_2^2 - p_3^2 > p_3^2 - p_4^2$. Thus, leakage is easily detected by monitoring the ratios between the squared pressure differences.

Once leakage is detected, the location of leakage can be determined using the linearity of p^2 along a simple pipeline in Eq. (13). For the situation shown in Fig. 3, the leakage position can be determined as the intersection point of two lines: $p_1^2 + (p_2^2 - p_1^2)x/S$ and $p_3^2 + (p_4^2 - p_3^2)(x - 2S)/S$.

In summary, the pressure differential monitoring with four equally-spaced pressure sensors, p_1, p_2, p_3, and p_4, can be stated as

$$\text{Detection: } \frac{p_1^2 - p_2^2}{p_2^2 - p_3^2} \text{ and } \frac{p_2^2 - p_3^2}{p_3^2 - p_4^2} > \text{TOL}, \tag{14}$$

$$\text{Location: } \frac{x_{\text{leak}}}{S} = \frac{p_1^2 - 3p_3^2 + 2p_4^2}{p_1^2 - p_2^3 - p_3^2 + p_4^2}, \tag{15}$$

where TOL is the tolerance for leakage judgment.

3. Results

3.1 Model validation

The reliability of the present pipeline simulation model was checked by solving a validation problem in Emara-Shabaik et al. [13]. This problem is related to a transient situation in which the supply pressure is suddenly increased to $p_s + \Delta p_s$ during a simple pipeline branch is operated steadily with supply pressure of p_s and demand pressure p_d. Fluid properties, geometric parameters, and operation conditions are summarized in Table 1. In the calculation, the steady state results obtained from $p_s = 1.5$ bar and $p_d = 1.0$ bar were used as the initial conditions.

Fig. 4(a) shows the transient pressure histories at three positions of $L/4$, $L/2$, and $3L/4$ in the simple pipeline due to an abrupt increase of supply pressure. Fig. 4(b) shows the transient flow rate histories at the same positions. In both figures, lines denote the present results while symbols denote the results by Emara-Shabaik et al. [13]. The discrepancy between the two results is observed to be less than 1% for pressure and flow rate. Thus, the reliability and accuracy of the present pipeline simulation model is validated.

In Fig. 4, pressure in the simple pipeline branch is observed as having reached a new steady state corresponding to the increased supply pressure of 3.5 bar at about 2500 s. Due to the long pipeline length of 90 km, sound wave requires 300 s to travel from one end to the other. Thus, gas flow in the pipeline requires about ten times longer transient time to reach a new steady state upon abrupt change of BCs. The flow rate in Fig. 4(b) does not always show monotonically increasing behaviors. Initially, the flow rate at $x = L/4$ rapidly increases, after which it slowly decreases to a steady flow rate. This behavior is believed be related to the compressibility of gas in pipelines.

Table 1. Physical parameters and operational conditions for the validation problem [13].

Parameters	Values
Pipeline length, L	90 km
Number of sub-sections, N	40
Pipe cross-sectional area, A	1 m^2
Density of gas, ρ_n	p_n / a^2 kg/m^3
Speed of sound, a	300 m/s
Pipe friction factor, f	0.003
Supply pressure, p_s	1.5 bar
Demand pressure, p_d	1.0 bar
Step increase of p_s, Δp_s	2.0 bar

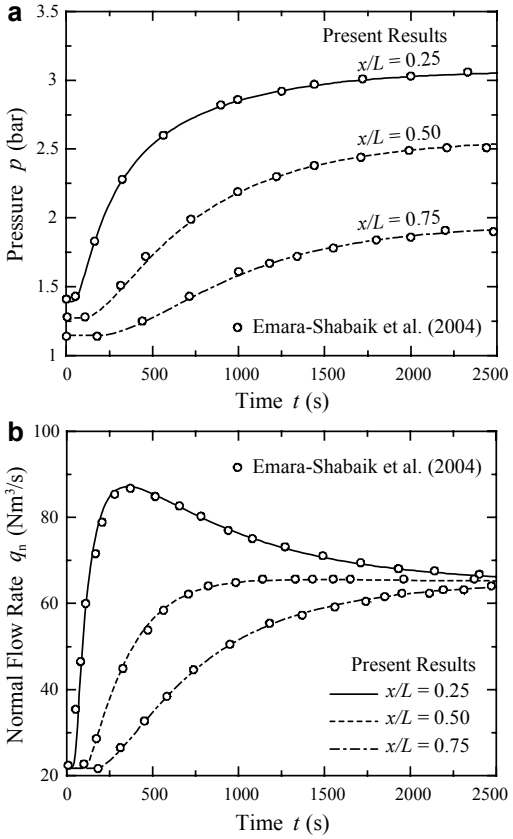

Fig. 4. Validation of the present pipeline simulation model in comparison with Emara-Shabaik et al. [13]: (a) pressure histories, and (b) flow rate histories.

3.2 Leakage simulation

Transient leakage simulation was performed by the validated pipeline model to numerically evaluate the two pipeline monitoring methods. Fig. 5 shows a sudden leakage situation

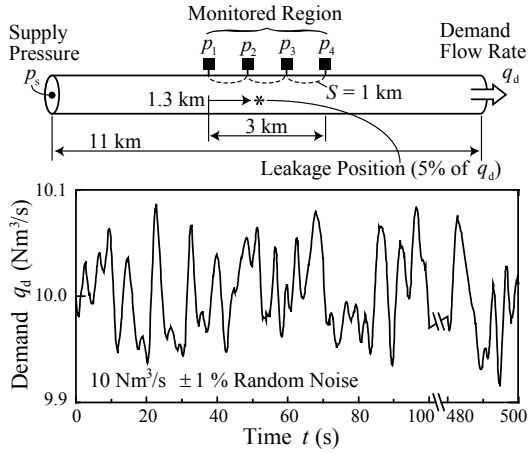

Fig. 5. Schematic diagram for the leakage problem considered in this study. Random fluctuation of ±1% magnitude is added to the demand flow rate for more realistic simulation.

occurring during steady state operation of a simple pipeline branch. The physical parameters and operation conditions for the leakage problem are summarized in Table 2. Note that the dimension of the pipeline branch was chosen from the actual dimension of pipes used for the mid-pressure range (2-8 bar in the absolute pressure) by local city-gas suppliers in Korea.

As shown in Fig. 5, four pressure sensors were assumed to be installed at uniform spacing S of 1 km in the middle monitored region of the 11-km long pipeline branch. The pipeline branch was assumed to be operated steadily at supply pressure p_s of 3 bar and demand flow rate q_d of 10 Nm^3/s. Random fluctuation of ±1% magnitude was added to q_d as shown in Fig. 5 for more realistic simulation. Leakage was assumed to occur at $t = 100$ s and $x_{leak} = 1.3$ km (x_{leak} denotes the leakage position measured from the first pressure sensor). Leakage rate q_{leak} was set as 5% of q_d. Transient simulation was conducted with a constant time step Δt of 0.1 s, which was also assumed as the sampling rate of pressure sensor signals.

Fig. 6 shows the simulated distribution of p and q_n in the middle region of the pipeline branch after leakage occurrence. In Fig. 6(a), pressure disturbance is observed to start from the leakage position at x_{leak} and propagate both upstream and downstream rapidly. After the fast initial variation, pressure in the whole region has decreased to a lower level, which corresponds to a new steady state, as shown in Fig. 6(a). Similarly, flow rate disturbance is also observed to begin at the leakage position, moving upstream and downstream in Fig. 6(b). The flow rate in the upstream region seems to experience a monotonic increase towards $q_d + q_{leak}$ (10.5 Nm^3/s). However, the flow rate in the downstream region has shown a fast decrease and a slow increase back to q_d (10 Nm^3/s).

Fig. 7 shows the transient histories of pressure p_i and pressure variation p_i' at the four sensor locations shown in Fig. 5. These histories were regarded as the transient signals recorded by the four pressure sensors at a sampling interval of 0.1 s (a sampling rate of 10 Hz). Fig. 7 shows that each pressure sensor signal has decreased to a new level due to abrupt leakage in the pipeline branch. By differentiating pressure signals in Fig. 7(a) with respect to time, the pressure variation histories can now be observed in Fig. 7(b). The second pressure sensor, p_2, has exhibited the largest pressure variation in magnitude since the leakage position is nearest to p_2. However, the other pressure sensors have shown similar behaviors in the pressure variations although their magnitudes are differ-

Table 2. Physical parameters and operational conditions for the leakage problem.

Parameters	Value
Pipeline length, L	11 km
Number of sub-sections, N	110
Pipe diameter, D	0.4 m
Density of gas, ρ_n	p_n / a^2 kg/m^3
Speed of sound, a	356 m/s
Pipe friction factor, f	0.003
Supply pressure, p_s	3 bar
Demand flow rate, q_d	10 Nm^3/s
Leakage flow rate, q_{leak}	0.5 Nm^3/s
Leakage location (from first sensor), x_{leak}	1.3 km
Leakage time, t_{leak}	100 s

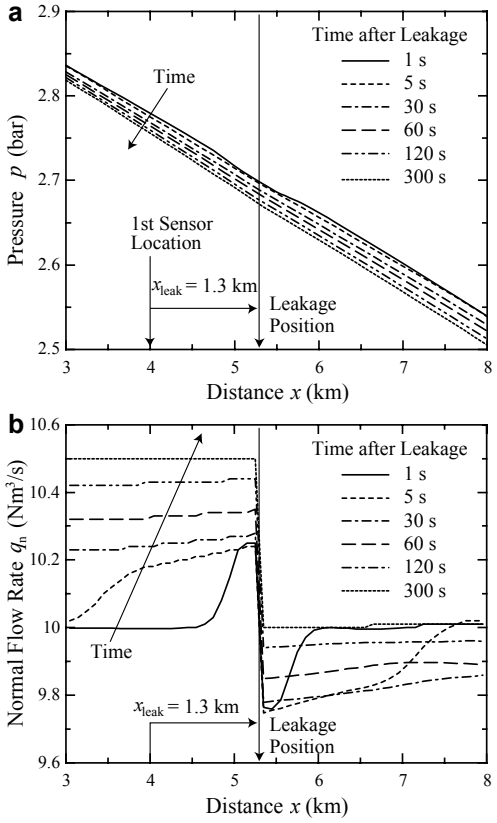

Fig. 6. Transient distributions in a simple pipeline branch after leakage: (a) pressure, and (b) flow rate distributions.

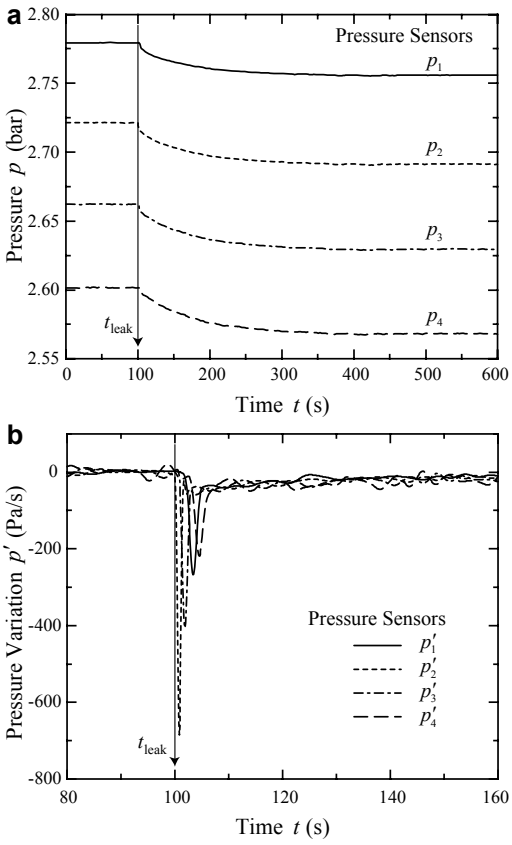

Fig. 7. Transient histories measured at the four pressure sensor locations: (a) pressure, and (b) pressure variation histories.

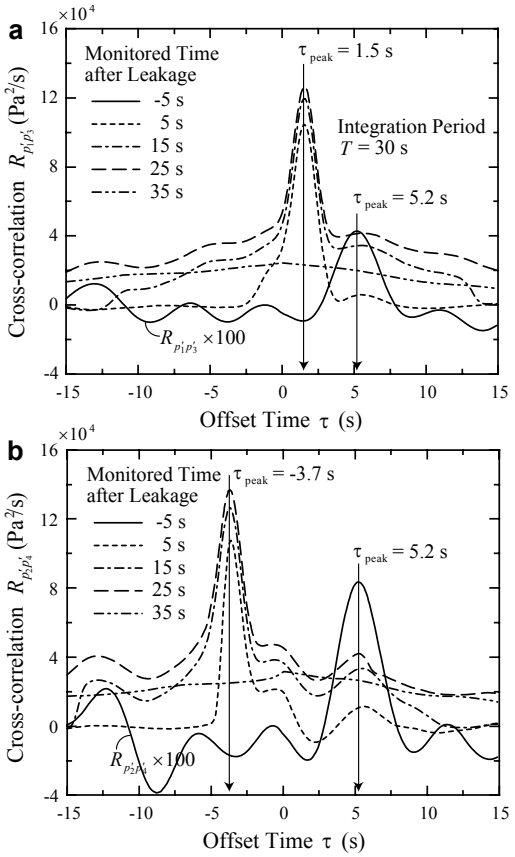

Fig. 8. Cross-correlation coefficients for pairs of two pressure sensor signals: (a) $p_1 - p_3$ sensors, and (b) $p_2 - p_4$ sensors.

ent according to the distance towards the leakage position.

3.3 Leakage detection and location

Numerical assessment of two monitoring methods was performed based on the simulated sensor signals shown in Fig. 7. First, the cross-correlation monitoring is considered. Fig. 8 shows the cross-correlation coefficients calculated with the pressure variation pairs of $p'_1 - p'_3$ and $p'_2 - p'_4$ shown in Fig. 7(b). Note that integration period T was set at 30 s; That is, the cross-correlation coefficients were calculated by Eq. (9) using pressure variation data recorded during the previous 30 s period (a total of 301 sampled data). In Fig. 8, it is observed that the peak value for $R_{p'_1p'_3}$ or $R_{p'_2p'_4}$ is obtained at $\tau = 2S/a \approx 5.2$ s before leakage. This is because most pressure disturbance signals are originated from the random ±1% fluctuation added to q_d at the downstream. In addition, the magnitude of $R_{p'_1p'_3}$ or $R_{p'_2p'_4}$ is generally small, as indicated in Fig. 8.

When leakage occurs, the magnitude of $R_{p'_1p'_3}$ or $R_{p'_2p'_4}$ is greatly increased. Peak offset time τ_{peak} correspondent to the maximum of $R_{p'_1p'_3}$ or $R_{p'_2p'_4}$ is also changed to a new value between $\pm 2S/a$. Such peak offset time can be attributed to the origin of abnormal pressure disturbances in the monitored region according to Eq. (12). In order to assess cross-correlation monitoring, the leakage detection method summarized in Eqs. (11) and (12) is tested in Fig. 9. As shown in Fig. 9(a), $\text{peak}[R_{p'_ip'_j}(\tau)]/\max[R_{p'_ip'_j}(\pm S_{ij}/a)]$ provides a good measure to detect leakage in the monitored region. Without leakage, this ratio is observed to remain near 1. However, with leakage in the monitored region, this ratio steeply increases and then remains higher than 2 while leakage timing t_{leak} is in the integration window of $T = 30$ s. Thus, leakage in a simple pipeline branch can be detected by properly setting TOL in Eq. (11).

The histories of peak offset time τ_{peak} are shown in Fig. 9(b). Once the occurrence of leakage in the monitored region is detected by the peak correlation ratio that is higher compared with TOL, the leakage position is determined based on Eq. (12). Fig. 9(b) shows that τ_{peak} relates to a constant value upon leakage detection. The leakage position is estimated to be 1.341 km for $R_{p'_1p'_3}$ and 1.290 km for $R_{p'_2p'_4}$, which results in only 10-40 m error for the two pressure sensors with 2 km spacing. Note that the leakage position can be more accurately estimated when $R_{p'_2p'_3}$ is calculated and analyzed.

The leakage detection and location by pressure differential monitoring, summarized in Eqs. (14) and (15), is numerically assessed in Fig. 10. While pressure variation data are used in cross-correlation monitoring, pressure differential monitoring uses pressure data for leakage detection. In Fig. 10(a), the

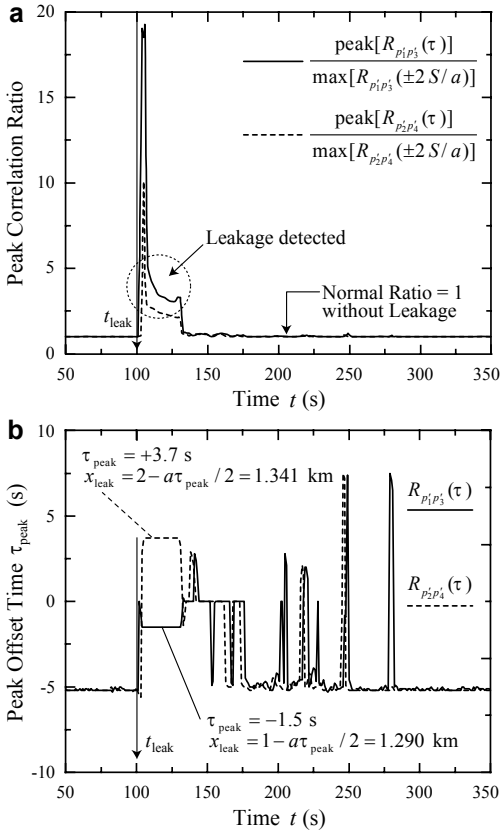

Fig. 9. Cross-correlation monitoring: histories of (a) peak correlation ratio, and (b) peak offset time.

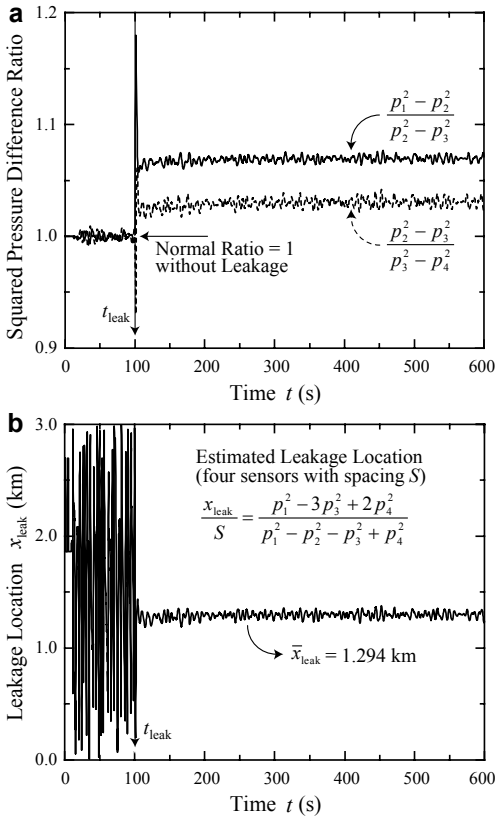

Fig. 10. Pressure differential monitoring: histories of (a) squared pressure difference ratio, and (b) estimated leakage location.

ratios of squared pressure differences are observed to remain constant around 1 without leakage in the monitored region, but increase to higher than 1 with leakage. The deviation of squared pressure difference ratios from 1 is relatively small (i.e., 1.07 and 1.03 in Fig. 10(a)). However, the systematic deviation is believed to be easily detected by integrating $(p_i^2 - p_{i+1}^2)/(p_{i+1}^2 - p_{i+2}^2) - 1$ for a certain proper period, T.

The leakage position estimated by pressure differential monitoring is shown in Fig. 10(b). It is observed that estimated leakage location x_{leak} fluctuates severely before the onset of actual leakage. One reason is that the denominator in Eq. (15) closes in to zero when without leakage. However, when leakage is present in the monitored region, x_{leak} converges to a constant value of 1.294 km, which results in only 6 m error for four pressure sensors with 1 km spacing.

4. Discussion

The present numerical study has shown the possibility of two simple methods based on an array of pressure sensors for the leakage monitoring of a gas pipeline branch. Thus, it would be meaningful to summarize the advantages and disadvantages of each monitoring method.

Cross-correlation monitoring provides a simple leakage detection and location irrespective of pipe dimensional change because the method is based only on signal processing without much reference to fluid mechanics. In addition, only two pressure sensors are required for leakage detection and location. However, cross-correlation monitoring cannot generally detect progressive leakage (slow increases of leakage rate) and requires processing of at least 200–300 sets of pressure variation data at a time. Note that pressure variation p' is obtained by differentiating p with respect to time and thus is more sensitive to measurement errors compared with p.

On the contrary, pressure differential methods can detect both abrupt and progressive leakages and require processing of only a single set of pressure data at a time. However, it requires special consideration for pipe dimensional change according to fluid mechanics, and requires at least four sensors for leakage detection and location. Thus, the two monitoring methods may be used complementary in the efficient detection and location of leakage in a simple pipeline branch.

Further studies are currently conducted to improve cross-correlation and pressure differential monitoring methods in order to enhance sensitivities to leakage detection, as well as to distinguish operational disturbances. In addition, studies are also being conducted to experimentally validate the two monitoring methods in a model pipeline branch.

5. Conclusions

In this study, two monitoring methods based on transient

signals from a pressure sensor array were numerically tested for leakage detection and location in simple pipeline branches. A pipeline simulation model was developed, validated, and used to obtain transient pressure sensor signals during the operation of a simple pipeline branch at a prescribed amount of leakage (5% of total flow rate in the pipeline branch). The obtained pressures and temporal pressure variations at the sensor locations were used to assess the capabilities of cross-correlation monitoring and pressure differential monitoring methods. Results demonstrated that both methods are useful in the detection and location of leakage in simple pipeline branches. The strong and weak points of each monitoring method were also discussed in detail.

Acknowledgment

This work was supported by New and Renewable Energy Research and Development Program (2007-M-CC23-P-03-1-000) under Korea Ministry of Commerce, Industry, and Energy (MOCIE).

Nomenclature

a : Speed of sound, m/s
f : Darcy friction factor
L : Length of pipeline branch, m
p : Pressure, Pa
p' : Pressure variation, Pa/s
p_n : Standard pressure, 1 bar
q : Flow rate, m^3/s
q_n : Normalized flow rate, Nm^3/s
q_{leak} : Normalized leakage rate, Nm^3/s
$R_{p'_1p'_2}$: Cross-correlation coefficient, Pa^2/s
S : Sensor spacing, m
T_n : Standard temperature, 288 K
τ : Offset time, s
x_{leak} : Leakage position, m

References

[1] A. Benkherouf and A. Y. Allidina, Leak detection and location in gas pipelines, *IEE Proc. D,* 135 (1988) 142-148.
[2] J. Zhang, Designing a cost effective and reliable pipeline leak detection system, *Pipes & Pipeline Int.,* 42 (1997) 20-26.
[3] I. Brodetsky and M. Savic, Leak monitoring system for gas pipeline, *IEEE International Conf. on Acoustics, Speech, and Signal Processing,* 3 (1993) 17-20.
[4] L. Billmann and R. Isermann, Leak detection methods for pipelines, *Automatica,* 23 (1987) 381-385.
[5] W. J. Turner and N. R. Mudford, Leak detection, timing, location and sizing in gas pipelines, *Math. Comput. Model.,* 10 (1988) 609-527.
[6] S. Belsito, P. Lombardi, P. Andreussi and S. Barerjce, 1998, Leak detection in liquefied gas pipelines by artificial neural network, *AIChE J.,* 44 (1998) 2675-2688.
[7] K. Fukushima, R. Maeshima, A. Kinoshita, H. Shiraishi and I. Koshijima, Gas pipeline leak detection system using the online simulation method, *Comput. Chem. Eng.,* 24 (2000) 453-456.
[8] A. C. Caputo and P. M. Pelagagge, An inverse approach for piping networks monitoring, *J. Loss Prevent. Proc. Ind.,* 15 (2002) 497-505.
[9] Y. J. Kim, K. Miyazaki and H. Tsukamoto, Leakage detection in pipe using transient flow and genetic algorithm, *J. Mech. Sci. Technol.,* 22 (2008) 1930-1936.
[10] I. Stoianov, L. Nachman, S. Madden and T. Tokmouline, PIPENET: A wireless sensor network for pipeline monitoring, *Proc. of Information, Processing in Sensor Networks*, (2007) 264-273.
[11] T. Kiuchi, An implicit method for transient gas flows in pipe networks, *Int. J. Heat Fluid Flow*, 15 (1994) 378-383.
[12] S. L. Ke and H. C. Ti, Transient analysis of isothermal gas flow in pipeline network, *Chem. Eng. J.,* 76 (2000) 169-177.
[13] H. E. Emara-Shabaik, Y. A. Khulief and I. Hussaini, Simulation of transient flow in pipelines for computer-based operations monitoring, *Int. J. Numer. Meth. Fluids*, 44 (2004) 257-275.
[14] C. Y. Cho, S. P. Jang, J. H. Nam, S. H. Lim, D. Shin and T. Y. Chung, A study on pipeline network analysis for predicting pressure and flow rate transients in city-gas supply lines, *KIGAS J.,* 12 (2008) 85-91.
[15] B. R. Munson, D. F. Young and T. H. Okiishi, *Fundamentals of Fluid Mechanics*, Third Ed., John Wiley & Sons, New York, USA. (1998).
[16] H. Siebert, A simple method for detecting and locating small leaks in gas pipelines, *Proc. Automat.,* 2 (1981) 90-95.
[17] C. Knapp and G. Carter, The generalized correlation method for estimation of time delay, *IEEE Trans. on Acoustics, Speech and Signal Processing,* 24 (1976) 320-327.
[18] R. Jamal and H. Pichlik, *LabVIEW. Applications and Solutions*, Prentice Hall, New Jersey, USA. (1999).

Sung Pill Jang received his B.S. degree in Mechanical Engineering from Kookmin University, Korea, in 2008. Currently, Mr. Jang is an M.S. student at the School of Mechanical and Automotive Engineering at Kookmin University in Seoul, Korea.

Jin Hyun Nam received his B.S., M.S., and Ph.D. degrees in Mechanical Engineering from Seoul National University, Korea, in 1996, 1998, and 2003, respectively. Dr. Nam currently works as an Assistant Professor at the School of Mechanical and Automotive Engineering at Kookmin University in Seoul, Korea. His research interests include fuel cell and battery systems, heat and mass transfer, and thermo-fluid process modeling.